NATIONAL ADVISORY COMMITTEE FOR AERONAUTICS

TECHNICAL NOTE

No. 1124

EFFECT OF SMALL DEVIATIONS FROM FLATNESS ON EFFECTIVE WIDTH AND BUCKLING OF PLATES IN COMPRESSION

By Pai C. Hu, Eugene E. Lundquist, and S. B. Batdorf

Langley Memorial Aeronautical Laboratory
Langley Field, Virginia

Washington
September 1946

NATIONAL ADVISORY COMMITTEE FOR AERONAUTICS

TECHNICAL NOTE No. 1124

EFFECT OF SMALL DEVIATIONS FROM FLATNESS ON EFFECTIVE WIDTH AND BUCKLING OF PLATES IN COMPRESSION

By Pai C. Hu, Eugene E. Lundquist, and S. B. Batdorf

SUMMARY

A theoretical investigation was undertaken to evaluate the effect of small deviations from flatness on the behavior of simply supported square plates under compression, it being assumed that the proportional limit is not exceeded. This study involved the solution of the von Kármán large-deflection equations according to the method used by Samuel Levy in NACA TN No. 846. As a result of the investigation, it was found that:

(1) The effects of initial deviations from flatness upon buckle growth and effective width of plate are most marked at stresses around the theoretical flat-plate critical stress; at stresses well above or below the critical stress, the behavior of a plate with an initial deviation from flatness is very much the same as that of an initially perfectly flat plate.

(2) In two commonly used laboratory methods giving experimental critical stresses related to the start of rapidly increasing lateral deflections it may be expected that the larger the initial deviation from flatness the smaller is the experimental critical stress.

(3) The Southwell plot method of predicting theoretical critical stresses for perfect specimens from experimental observations on actual specimens may not be expected to give, in general, satisfactory results when applied to flat plates.

INTRODUCTION

Flat and curved plates constitute basic structural elements in an all-metal airplane structure. The behavior and strength of both types of plate for various loading conditions have been treated in the literature in varying degrees.

The flat plate under compression has been treated very extensively in previous work, but almost always with the restriction that the plate be perfectly flat. In experimental studies of the compressive strength of stiffeners and stiffened panels that consist of flat-plate elements, the so-called flat plates have been found to behave not as perfectly flat plates, for which buckles begin to form at a definite load called the critical load, but to behave rather as plates with slight deviations from flatness, for which buckles begin to grow with the beginning of loading. The rate at which the buckles grow with increase in load is very slow at first but increases appreciably as the critical load is approached, after which the rate of buckle growth with load gradually diminishes.

Since every flat plate in practical use behaves as a plate with slight deviations from flatness, a theoretical study of simply supported square plates under compression was undertaken to evaluate the effect of small deviations from flatness on

(1) Growth of buckles with increase in load

(2) Effective width of plate

(3) Experimentally determined buckling or critical stress

(4) Applicability of the Southwell plot method of predicting theoretical critical stresses for perfectly flat plates from experimental observations on actual plates

The present study involved the solution of the von Kármán large-deflection equations according to the method of Samuel Levy (reference 1) in order to obtain simulated test data for plates with several initial deviations from flatness.

The mathematical development of the equations required for the present investigation is given in appendix A for a rectangular plate under lateral pressure and longitudinal and transverse compression. In appendix B the special case of a square plate subjected to compression in only one direction is treated. Throughout the investigation the assumption is made that the stresses remain below the proportional limit.

SYMBOLS

The coordinate system is shown in figure 10.

a plate length in x-direction

b plate length in y-direction

b_e effective width for load-carrying capacity

b'_e effective width for stiffness against further edge compression

D flexural rigidity $\left(\frac{Et^3}{12(1-\mu^2)}\right)$

E Young's modulus

F stress function

k positive integer used as subscript

K_{mn} dimensionless deflection coefficient $\left(\frac{w_{mn}}{t}\right)$

$K_{o_{mn}}$ dimensionless coefficient for initial deflection $\left(\frac{w_{o_{mn}}}{t}\right)$

m,n,p positive integers used as subscripts

p_{rs} coefficients in infinite series for p_z

p_z normal pressure

q,r,s,t	positive integers used as subscripts
t	plate thickness
u,v,w	deflections of a point in the x-, y-, and z-directions, respectively
w_o	initial deflection in z-direction
w_{mn}	coefficients in infinite series for w
$w_{o_{mn}}$	coefficients in infinite series for w_o
x,y,z	coordinates of a point measured from origin at corner of plate (see fig. 10)
γ_{xy}	shearing strain
γ'_{xy}	shearing strain in middle surface
δ	total deflection at center of plate
δ_o	initial deflection at center of plate
$\bar{\epsilon}_a$	unit plate shortening in x-direction (total shortening divided by a)
$\bar{\epsilon}_b$	unit plate shortening in y-direction (total shortening divided by b)
ϵ_x, ϵ_y	compressive strain in x- and y-directions, respectively
ϵ'_x, ϵ'_y	middle-surface compressive strain in x- and y-directions, respectively
ϵ_1	extreme-fiber compressive strain in x-direction at concave side of plate center
ϵ_2	extreme-fiber compressive strain in x-direction at convex side of plate center
ϵ_{cr_x}	critical strain in x-direction for a flat plate subjected to compressive stress in x-direction
μ	Poisson's ratio
σ_a	edge compressive stress in x-direction
σ_b	edge compressive stress in y-direction

$\bar{\sigma}_a$ average edge compressive stress in x-direction

$\bar{\sigma}_b$ average edge compressive stress in y-direction

σ_x, σ_y compressive stresses in x- and y-directions, respectively

σ'_x, σ'_y middle-surface compressive stresses in x- and y-directions, respectively

σ''_x, σ''_y extreme-fiber compressive bending stresses in x- and y-directions, respectively

σ_{cr_x} critical edge compressive stress in x-direction for a flat plate $\left(\left[\frac{E\pi^2 t^2}{3(1-\mu^2)b^2}\right]$ for a square plate$\right)$

τ_{xy} shearing stress

τ'_{xy} shearing stress in middle surface

τ''_{xy} extreme-fiber shearing stress due to bending only

Deviations from Flatness Considered

The types of initial curvature, deviations from flatness, selected for the numerical analysis are those components of the buckle pattern that first become predominant after the assumed-flat square plate buckles.

Let the deflection surface of the simply supported square plate be represented by the equation

$$w = \sum_{m=1}^{\infty} \sum_{n=1}^{\infty} w_{mn} \sin \frac{m\pi x}{b} \sin \frac{n\pi y}{b}$$

$$= t \sum_{m=1}^{\infty} \sum_{n=1}^{\infty} K_{mn} \sin \frac{m\pi x}{b} \sin \frac{n\pi y}{b}$$

where the absolute value of w_{mn} is the amplitude of a

component deflection surface with m half waves in the x-direction and n half waves in the y-direction, and K_{mn} is a nondimensional measure of w_{mn} in terms of the plate thickness $\left(K_{mn} = \frac{w_{mn}}{t}\right)$.

At zero load the deflection surface w_o, which describes the initial deviation from flatness, is given as

$$w_o = t \sum_{m=1}^{\infty} \sum_{n=1}^{\infty} K_{o_{mn}} \sin \frac{m\pi x}{b} \sin \frac{n\pi y}{b}$$

$$\left(K_{o_{mn}} = 0 \text{ for perfectly flat plate}\right)$$

When a simply supported, perfectly flat square plate first buckles, the deflection surface w is of the form

$$tK_{11} \sin \frac{\pi x}{b} \sin \frac{\pi y}{b}$$

but as the deflection increases, other components appear, the most important of which is

$$tK_{31} \sin \frac{3\pi x}{b} \sin \frac{\pi y}{b}$$

It is therefore reasonable to assume that

$$tK_{o_{11}} \sin \frac{\pi x}{b} \sin \frac{\pi y}{b}$$

and

$$tK_{o_{31}} \sin \frac{3\pi x}{b} \sin \frac{\pi y}{b}$$

are the two most important types of initial deviation from flatness. Since the first of these types has a greater effect than the second, more variations were studied of the first than of the second. The particular combinations of initial curvature of the $K_{o_{11}}$ and $K_{o_{31}}$ type considered for numerical computation are given in the following table:

$K_{o_{11}}$	$K_{o_{31}}$
0	0 (flat)
.01	0
.04	0
.10	0
0	.01
.04	.01

RESULTS AND DISCUSSION

The assumption is made in the analysis that all edges of the plate remain straight when buckling occurs, and that the side edges are allowed to translate in the plane of the plate to such a position that the resultant of the transverse forces on the side edges of the plate is zero. The edge positions and stress distribution corresponding to such an assumption for an initially perfectly flat plate are indicated in figure 1. When the plate is not perfectly flat the stress distributions are, from the beginning of loading, more or less of the general type illustrated by the "after-buckling" case shown in figure 1.

The theoretical study of the effect of deviations from flatness on

(1) Growth of buckles with increase in load

(2) Effective width of plate

(3) Experimentally defined buckling or critical stress

(4) Applicability of Southwell plot method of predicting theoretical critical stresses for perfectly flat plates from experimental observations on actual plates

disclosed relationships which would be of most general value when presented in nondimensional form by the use of such natural ratios as $\frac{\delta - \delta_o}{t}$, $\frac{\bar{\sigma}_a}{\sigma_{cr_x}}$, $\frac{\bar{\epsilon}_a}{\epsilon_{cr_x}}$, $\frac{b_e}{b}$, and $\frac{b'_e}{b}$. Poisson's ratio μ is taken as 0.316 for the computations. The computed results apply only if the proportional limit is not exceeded.

Growth of Buckles with Increase in Load

The way in which the net center deflection $\delta - \delta_o$ increases with load as measured by the average stress $\bar{\sigma}_a$ is shown in figure 2. When a perfectly flat plate is subjected to an increasing edge compression, no deflection of the plate out of its original plane occurs until a definite stress, called the critical stress, is reached. An increase in load above the critical load causes large deflections which grow less and less rapidly as the load increases more and more. (See curve for $K_{o_{11}} = K_{o_{31}} = 0$ in fig. 2.)

When a plate with an initial deviation from flatness is subjected to compression, the deflections that result from application of load grow very slowly with the first increments of load but grow very rapidly as the critical load is approached; near the critical load the rate of increase of $\delta - \delta_o$ with further increase in load diminishes and $\delta - \delta_o$ approaches the deflection for the perfectly flat plate at values not far above the critical load. (See curves other than $K_{o_{11}} = K_{o_{31}} = 0$ in fig. 2.)

Effective Width of Plate

The fundamental information for evaluating the effect of deviations from flatness on two types of effective width of plate is presented in figure 3 where the ratio of average stress to critical stress $\bar{\sigma}_a/\sigma_{cr_x}$ is plotted against the ratio of unit plate shortening to critical strain $\bar{\epsilon}_a/\epsilon_{cr_x}$.

The usual "effective width" b_e, which is associated with the load-carrying capacity of the plate, may be defined (see last paragraph of appendix B for derivation) by the equation

$$b_e = b\frac{\bar{\sigma}_a/\sigma_{cr_x}}{\bar{\epsilon}_a/\epsilon_{cr_x}}$$

Thus the ratio of the effective width for load-carrying capacity to the actual width of the plate b_e/b is equal to the ratio of ordinate to abscissa in figure 3. In figure 4 the effective-width ratio b_e/b for load-carrying capacity is plotted against the ratio of average stress to critical stress $\bar{\sigma}_a/\sigma_{cr_x}$ for plates with different amounts of initial deviation from flatness.

Another type of "effective width" b'_e is associated with the stiffness of the plate against further compression (that is, $d\bar{\sigma}_a/d\bar{\epsilon}_a$), and is defined by the equation

$$\frac{b'_e}{b} = \frac{d\left(\bar{\sigma}_a/\sigma_{cr_x}\right)}{d\left(\bar{\epsilon}_a/\epsilon_{cr_x}\right)}$$

(A detailed discussion of this type of effective width is contained in reference 2 where it is referred to as "reduced effective width.") Thus the ratio of effective

width for stiffness to actual width b'_e/b is given directly by the slope of a curve of $\bar{\sigma}_a/\sigma_{cr_x}$ against $\bar{\epsilon}_a/\epsilon_{cr_x}$. Such curves are shown in figure 3 for plates with different amounts of initial deviation from flatness. In figure 5, the effective-width ratio for stiffness b'_e/b is plotted against the ratio of average stress to critical stress $\bar{\sigma}_a/\sigma_{cr_x}$.

The effects of initial deviations from flatness upon the effective width of simply supported square plates are most marked at stresses around the theoretical flat-plate critical stress. The effective width for load-carrying capacity of a plate with an initial deviation from flatness is, at all values of stress, less than that of an initially perfectly flat plate (fig. 4). The effective width for stiffness against further compression, however, is less than that of a flat plate at stresses below the theoretical critical stress but greater at stresses above the critical (fig. 5). At stresses well above or below the critical stress the effect of initial deviations upon either effective width of plate becomes negligible.

Experimentally Defined Buckling or Critical Stress

Since buckles begin to grow with the beginning of loading for a plate that has an initial deviation from flatness, there can be no buckling stress for an actual plate in the strict theoretical sense; however, just as a defined yield stress has been found useful for materials that have no actual yield stress, so a defined buckling or critical stress for a plate can convey much meaning to a practicing engineer.

A perfectly flat plate remains flat until the buckling stress is reached, whereupon buckles are produced that grow rapidly with very small further increases in load. (See curve labeled $K_{o_{11}} = K_{o_{31}} = 0$ in fig. 2.) Since the rapid increase of lateral deflection with load is an important aspect of the buckling of a perfectly flat plate, it is reasonable to retain this concept as the

basis of an experimentally determined buckling stress for an actual plate. Because, however, strains are usually more easily measured than deflections with the equipment available at present and because the manner of growth of the extreme-fiber strains at either side of the buckle crest is indicative of the increase in lateral deflections, these strains instead of the lateral deflections are frequently measured in determining the buckling stresses of plates.

In two NACA papers on the compressive strength of stiffened panels (references 3 and 4) a method that will be referred to herein as the "strain-reversal method" has been used to obtain experimental buckling stresses. The critical stress obtained by this method is defined as the stress at which the extreme-fiber strain ϵ_2 on the convex side of the buckle crest stops increasing and begins to decrease. Critical stresses obtained according to this definition are indicated by circles in figure 6, where the calculated extreme-fiber strains in the direction of loading at either side of the buckle crest are plotted as the abscissa against the average applied stress as the ordinate for plates with various assumed initial deviations from flatness.

In a series of NACA papers on the plate compressive strength of metals (references 5 to 10), the experimental buckling stress was determined by a method that will be referred to herein as the "top-of-the-knee method." The critical stress, according to this method, is essentially the stress corresponding to the top of the knee of a curve of stress against lateral deflection. If the lateral deflections cannot be readily measured, any other quantity that increases in substantially the same manner as the lateral deflections may be plotted instead. One such quantity is $\epsilon_1 - \epsilon_2$, the difference in strains in the direction of loading at the two sides of the buckle crest. Buckling stresses obtained by the top-of-the-knee method are indicated by squares on the curves of figure 7 for the several assumed initial deviations from flatness considered in the present paper.

The critical stresses obtained by the two methods just described are shown transferred to the stress-deflection curves of figure 8. Both methods give critical stresses that lie roughly on the knee of the stress-deflection curve, the strain-reversal critical stress

being the more conservative of the two. Since the knee of the curve may be judged to be the transition stage from a low to a high rate of increase of lateral deflection with load, both methods can be considered appropriate for obtaining experimental buckling stresses, according to the criterion adopted herein as the basis for defining an experimental buckling stress. Regardless of which method is used, a certain degree of personal judgment must be exercised in the selection of the buckling stresses, and the experimentally obtained buckling stress becomes more and more uncertain as the initial deviation from flatness increases. Despite this uncertainty, it is clear that the effect of initial deviations is to reduce the experimentally determined buckling stress.

Critical Stress and Postbuckling Behavior of Plate

The experimental definitions of critical stress just discussed were based on the concept of rate of growth of lateral deflection with load as the theoretical critical stress is approached. Since the rate of growth of lateral deflections below the theoretical critical stress is strongly influenced by the initial deviation from flatness, it is natural and perhaps desirable that any method for determining experimental critical stresses should be sensitive to initial deviations from flatness.

At stresses considerably beyond the buckling stress, however, the behavior of the plate is essentially independent of initial deviations from flatness. (See figs. 2 to 7.) For describing the elastic plate behavior in this range of stress, it is therefore advantageous to use, if possible, the theoretical critical stress, which is also independent of the initial imperfections of the plate.

Southwell Plot Method of Predicting Theoretical Critical Stress

Because the critical stresses for perfect specimens are valuable both for checking theories and predicting postbuckling behavior and because in many cases such

critical stresses are difficult to compute, a method of determining them from experimental data on imperfect specimens appears to be very desirable. Southwell has produced such a method for columns (reference 11), which has been modified in reference 12 for easier application to experimental work. Although this method applies to flat plates under compression according to small-deflection theory (p. 321 of reference 13) it has been found somewhat unsatisfactory for general use in the laboratory.

An essential requirement for the success of the Southwell method is that at least a part of the stress-deflection curve approximate a rectangular hyperbola

$$\frac{\delta}{t}\left(1 - \frac{\bar{\sigma}_a}{\sigma_{cr_x}}\right) = \frac{\delta_o}{t} \qquad \text{(for simply supported plates)}$$

$$\frac{\delta}{t}\left(1 - \frac{\bar{\sigma}}{\sigma_{cr}}\right) = \frac{\delta_o}{t} \qquad \text{(for pin-ended columns)}$$

where δ is the total deflection of the center of the column or plate, δ_o is the initial deflection of the center of the column or plate, $\bar{\sigma}$ is the average compressive stress on a column, and σ_{cr} is the critical compressive stress. The test data from which the Southwell plot is constructed must then be taken from this part of the curve. In the light of this requirement, the reason for the success of the Southwell method when applied to columns and for its failure when applied to plates is made clear in figure 9, where the stress-deflection curves for simply supported columns and plates are compared with the rectangular hyperbolas that they must approximate. (The stress-deflection curve in fig. 9(b) is for a column of which the initial shape is a circular arc and was calculated by large-deflection theory by a method similar to that used on pp. 69 to 72 of reference 13.) In the case of a column, regardless of the initial shape, the requirement that a part of the stress-deflection curve approximate a rectangular hyperbola is certain to be met as the stress approaches the critical value. In the case of a plate, however, the stress-deflection curve usually

does not approximate a rectangular hyperbola at stresses near the critical stress unless the initial deviation from flatness happens to be very small (fig. 9(a)). Experience in the structures research laboratory of the NACA Langley Laboratory indicates that the initial deviation from flatness and the inevitable inaccuracy of loading are usually not sufficiently small to guarantee this close approximation. Even if these factors are sufficiently small, difficulty is encountered in measuring with sufficient accuracy the very small strains or deflections used to make the Southwell plot for this special case.

The close agreement between the plate stress-deflection curves and the rectangular hyperbolas at low values of stress (fig. 9(a)) is largely fortuitous and occurs because the type of initial deviation from flatness assumed is the same as the lowest buckling mode.

CONCLUSIONS

The following conclusions are based on an analysis of simulated test data calculated by large-deflection theory and apply to the elastic behavior of simply supported square plates under compression.

1. The effects of initial deviations from flatness upon the buckle growth and effective width of simply supported square plates are most marked at stresses around the theoretical flat-plate critical stress. At stresses well above or below the critical stress the behavior of a plate with an initial deviation from flatness is very much the same as that of an initially perfectly flat plate.

2. The effective width for load-carrying capacity of a plate with an initial deviation from flatness is, at all values of stress, less than that of an initially perfect plate. The effective width for stiffness against further compression, however, is less than that of a flat plate at stresses below the theoretical critical stress but greater at stresses above.

3. Either of two commonly used laboratory methods, the strain-reversal method and the top-of-the-knee method, gives experimental critical stresses that are lower than

the theoretical flat-plate critical stress, the strain-reversal method generally giving more conservative values than the top-of-the-knee method. Such experimental critical stresses are significant as an indication of the start of rapidly growing lateral deflections. The effect of increasing the initial deviation from flatness is to reduce the experimental critical stress as determined by either method.

4. The Southwell plot method of predicting theoretical critical stresses for perfect specimens from experimental observations on actual specimens may not be expected to give, in general, satisfactory results when applied to flat plates.

Langley Memorial Aeronautical Laboratory
National Advisory Committee for Aeronautics
Langley Field, Va., May 13, 1946

APPENDIX A

SOLUTION OF VON KÁRMÁN EQUATIONS

The differential equations derived by von Kármán for the equilibrium of a flat rectangular plate under the action of normal pressure p_z and central surface stresses described by the stress function F are as follows (reference 1):

$$\frac{\partial^4 F}{\partial x^4} + 2\frac{\partial^4 F}{\partial x^2 \partial y^2} + \frac{\partial^4 F}{\partial y^4} = E\left[\left(\frac{\partial^2 w}{\partial x \partial y}\right)^2 - \frac{\partial^2 w}{\partial x^2}\frac{\partial^2 w}{\partial y^2}\right] \qquad (A1)$$

$$\frac{\partial^4 w}{\partial x^4} + 2\frac{\partial^4 w}{\partial x^2 \partial y^2} + \frac{\partial^4 w}{\partial y^4} = \frac{p_z}{D}$$

$$+ \frac{t}{D}\left(\frac{\partial^2 F}{\partial y^2}\frac{\partial^2 w}{\partial x^2} + \frac{\partial^2 F}{\partial x^2}\frac{\partial^2 w}{\partial y^2} - 2\frac{\partial^2 F}{\partial x \partial y}\frac{\partial^2 w}{\partial x \partial y}\right) \qquad (A2)$$

(The coordinate system is shown in fig. 10.)

If the plate has an initially curved surface described by the function w_o, the strains used to establish equation (A1) must be revised as follows:

Strains	Flat plate	Initially curved plate
$-\epsilon_x$	$\frac{\partial u}{\partial x} + \frac{1}{2}\left(\frac{\partial w}{\partial x}\right)^2$	$\frac{\partial u}{\partial x} + \frac{1}{2}\left(\frac{\partial w}{\partial x}\right)^2 - \frac{1}{2}\left(\frac{\partial w_o}{\partial x}\right)^2$
$-\epsilon_y$	$\frac{\partial v}{\partial y} + \frac{1}{2}\left(\frac{\partial w}{\partial y}\right)^2$	$\frac{\partial v}{\partial y} + \frac{1}{2}\left(\frac{\partial w}{\partial y}\right)^2 - \frac{1}{2}\left(\frac{\partial w_o}{\partial y}\right)^2$
γ_{xy}	$\frac{\partial u}{\partial y} + \frac{\partial v}{\partial x} + \frac{\partial w}{\partial x}\frac{\partial w}{\partial y}$	$\frac{\partial u}{\partial y} + \frac{\partial v}{\partial x} + \frac{\partial w}{\partial x}\frac{\partial w}{\partial y} - \frac{\partial w_o}{\partial x}\frac{\partial w_o}{\partial y}$

The left side of equation (A2) is obtained from expressions for bending and twisting moments; and, since the moments depend not on the total curvature but only on the change in curvature of the plate, the net deflection $w - w_o$ instead of the total deflection w should be used on the left side for an initially curved plate. The right side of equation (A2) gives the combined effect of the lateral load p_z and forces in the plane of the plates; and, since the effect of the forces in the plane of the plates depends on the total deflection w, the right side of equation (A2) remains unchanged for an initially curved plate.

The equations of equilibrium for an initially curved plate therefore become

$$\frac{\partial^4 F}{\partial x^4} + 2\frac{\partial^4 F}{\partial x^2 \partial y^2} + \frac{\partial^4 F}{\partial y^4} = E\left[\left(\frac{\partial^2 w}{\partial x \partial y}\right)^2 - \frac{\partial^2 w}{\partial x^2}\frac{\partial^2 w}{\partial y^2} - \left(\frac{\partial^2 w_o}{\partial x \partial y}\right)^2 + \frac{\partial^2 w_o}{\partial x^2}\frac{\partial^2 w_o}{\partial y^2}\right] \quad (A3)$$

$$\frac{\partial^4 (w - w_o)}{\partial x^4} + 2\frac{\partial^4 (w - w_o)}{\partial x^2 \partial y^2} + \frac{\partial^4 (w - w_o)}{\partial y^4} = \frac{p_z}{D} + \frac{t}{D}\left(\frac{\partial^2 F}{\partial y^2}\frac{\partial^2 w}{\partial x^2} + \frac{\partial^2 F}{\partial x^2}\frac{\partial^2 w}{\partial y^2} - 2\frac{\partial^2 F}{\partial x \partial y}\frac{\partial^2 w}{\partial x \partial y}\right) \quad (A4)$$

The middle-surface stresses are

$$\left.\begin{aligned} \sigma'_x &= -\frac{\partial^2 F}{\partial y^2} \\ \sigma'_y &= -\frac{\partial^2 F}{\partial x^2} \\ \tau'_{xy} &= -\frac{\partial^2 F}{\partial x \partial y} \end{aligned}\right\} \quad (A5)$$

The middle-surface strains are

$$\left.\begin{aligned} -\epsilon'_x &= \frac{1}{E}\left(\frac{\partial^2 F}{\partial y^2} - \mu\frac{\partial^2 F}{\partial x^2}\right) \\ -\epsilon'_y &= \frac{1}{E}\left(\frac{\partial^2 F}{\partial x^2} - \mu\frac{\partial^2 F}{\partial y^2}\right) \\ \gamma'_{xy} &= -\frac{2(1+\mu)}{E}\frac{\partial^2 F}{\partial x \partial y} \end{aligned}\right\} \qquad (A6)$$

The extreme-fiber bending and shearing stresses due to bending alone are

$$\left.\begin{aligned} \sigma''_x &= \pm\frac{Et}{2(1-\mu^2)}\left[\frac{\partial^2(w-w_o)}{\partial x^2} + \mu\frac{\partial^2(w-w_o)}{\partial y^2}\right] \\ \sigma''_y &= \pm\frac{Et}{2(1-\mu^2)}\left[\frac{\partial^2(w-w_o)}{\partial y^2} + \mu\frac{\partial^2(w-w_o)}{\partial x^2}\right] \\ \tau''_{xy} &= \pm\frac{Et}{2(1+\mu)}\frac{\partial^2(w-w_o)}{\partial x \partial y} \end{aligned}\right\} \qquad (A7)$$

A solution of equations (A3) and (A4) must satisfy the boundary conditions that the deflection and the bending moment per unit length along the edges be zero:

At $x = 0$ and $x = a$,

$$\frac{\partial^2(w - w_o)}{\partial x^2} + \mu\frac{\partial^2(w - w_o)}{\partial y^2} = 0$$

At $y = 0$ and $y = b$,

$$\frac{\partial^2(w - w_o)}{\partial y^2} + \mu\frac{\partial^2(w - w_o)}{\partial x^2} = 0$$

These conditions are satisfied by the two Fourier series

$$\left.\begin{aligned} w &= \sum_{m=1}^{\infty}\sum_{n=1}^{\infty} w_{mn} \sin\frac{m\pi x}{a} \sin\frac{n\pi y}{b} \\ w_o &= \sum_{m=1}^{\infty}\sum_{n=1}^{\infty} w_{o_{mn}} \sin\frac{m\pi x}{a} \sin\frac{n\pi y}{b} \end{aligned}\right\} \qquad (A8)$$

The normal pressure may be expressed by the Fourier series

$$p_z = \sum_{r=1}^{\infty}\sum_{s=1}^{\infty} p_{rs} \sin\frac{r\pi x}{a} \sin\frac{s\pi y}{b} \qquad (A9)$$

By substitution, equation (A3) is found to be satisfied if

$$F = -\frac{\bar{\sigma}_a y^2}{2} - \frac{\bar{\sigma}_b x^2}{2} + \sum_{p=0}^{\infty}\sum_{q=0}^{\infty} \left(b_{pq} - b_{o_{pq}}\right) \cos\frac{p\pi x}{a} \cos\frac{q\pi y}{b} \qquad (A10)$$

where $\bar{\sigma}_a$ and $\bar{\sigma}_b$ are the average applied stresses in the x- and y-directions, respectively, and where

$$b_{pq} = \frac{E}{4\left(p^2\frac{b}{a} + q^2\frac{a}{b}\right)^2} \sum_{n=1}^{9} B_n$$

and

$$B_1 = \sum_{k=1}^{p-1} \sum_{t=1}^{q-1} \left[kt(p - k)(q - t) - k^2 (q - t)^2\right] w_{kt}\, w_{(p-k)(q-t)}$$

if $q \neq 0$ and $p \neq 0$

$B_1 = 0$, if $p = 0$ or $q = 0$

$$B_2 = \sum_{k=1}^{\infty} \sum_{t=1}^{q-1} \left[kt(k + p)(q - t) + k^2 (q - t)^2\right] w_{kt}\, w_{(k+p)(q-t)}$$

if $q \neq 0$

$B_2 = 0$, if $q = 0$

$$B_3 = \sum_{k=1}^{\infty} \sum_{t=1}^{q-1} \left[(k + p)\, tk\, (q - t) + (k + p)^2 (q - t)^2\right] w_{(k+p)t}\, w_{k(q-t)}$$

if $q \neq 0$ and $p \neq 0$

$B_3 = 0$, if $q = 0$ or $p = 0$

$$B_4 = \sum_{k=1}^{p-1} \sum_{t=1}^{\infty} \left[kt(p - k)(t + q) + k^2 (t + q)^2 \right] w_{kt}\, w_{(p-k)(t+q)}$$

if $p \neq 0$

$B_4 = 0$, if $p = 0$

$$B_5 = \sum_{k=1}^{p-1} \sum_{t=1}^{\infty} \left[k(t + q)(p - k)t + k^2 t^2 \right] w_{k(t+q)}\, w_{(p-k)t}$$

if $q \neq 0$ and $p \neq 0$

$B_5 = 0$, if $q = 0$ or $p = 0$

$$B_6 = \sum_{k=1}^{\infty} \sum_{t=1}^{\infty} \left[kt(k + p)(t + q) - k^2 (t + q)^2 \right] w_{kt}\, w_{(k+p)(t+q)}$$

if $q \neq 0$ or $p \neq 0$

$B_6 = 0$, if $q = 0$ and $p = 0$

$$B_7 = \sum_{k=1}^{\infty} \sum_{t=1}^{\infty} \left[k(t + q)(k + p)t - k^2 t^2 \right] w_{k(t+q)}\, w_{(k+p)t}$$

if $q \neq 0$ and $p \neq 0$

$B_7 = 0$, if $q = 0$ or $p = 0$

$$B_8 = \sum_{k=1}^{\infty} \sum_{t=1}^{\infty} \left[(k + p)\,tk(t + q) - (k + p)^2\,(t + q)^2\right] w_{(k+p)t}\, w_{k(t+q)}$$

if $q \neq 0$ and $p \neq 0$

$B_8 = 0$, if $p = 0$ or $q = 0$

$$B_9 = \sum_{k=1}^{\infty} \sum_{t=1}^{\infty} \left[(k + p)(t + q)\,kt - (k + p)^2\,t^2\right] w_{(k+p)(t+q)}\, w_{kt}$$

if $p \neq 0$ or $q \neq 0$

$B_9 = 0$, if $p = 0$ and $q = 0$

$$b_{o_{pq}} = \frac{E}{4\left(p^2\frac{b}{a} + q^2\frac{a}{b}\right)^2} \sum_{n=1}^{q} B_{o_n}$$

The B_o terms are the same as the B terms except that w terms are replaced by w_o terms.

The terms b_{00} and $b_{o_{00}}$ may have any arbitrary value but they are of no importance because they vanish in the partial derivatives of the stress function F appearing in equations (A3) and (A4).

Equation (A4) is satisfied if

$$p_{rs} = D\left(w_{rs} - w_{o_{rs}}\right)\left(r^2\frac{\pi^2}{a^2} + s^2\frac{\pi^2}{b^2}\right)^2$$

$$- \overline{\sigma}_a t w_{rs} r^2 \frac{\pi^2}{a^2} - \overline{\sigma}_b t w_{rs} s^2 \frac{\pi^2}{b^2}$$

$$+ \frac{t\pi^4}{4a^2b^2}\left(A_{rs} - A_{o_{rs}}\right) \qquad \text{(A11)}$$

where

$$A_{rs} = \sum_{n=1}^{9} A_n$$

$$A_{o_{rs}} = \sum_{n=1}^{9} A_{o_n}$$

$$A_1 = -\sum_{k=1}^{r}\sum_{t=1}^{s} \left[(s - t)k - (r - k)t\right]^2 b_{(r-k)(s-t)} w_{kt}$$

$$A_2 = -\sum_{k=0}^{\infty}\sum_{t=0}^{\infty} \left[t(k + r) - k(t + s)\right]^2 b_{kt} w_{(k+r)(t+s)}$$

$$A_3 = \sum_{k=0}^{\infty} \sum_{t=1}^{\infty} [(k + r)(t + s) - kt]^2 \, b_{k(t+s)} \, w_{(k+r)t}$$

$$A_4 = \sum_{k=1}^{\infty} \sum_{t=0}^{\infty} [tk - (k + r)(t + s)]^2 \, b_{(k+r)t} \, w_{k(t+s)}$$

$$A_5 = - \sum_{k=1}^{\infty} \sum_{t=1}^{\infty} [(t + s)k - (k + r)t]^2 \, b_{(k+r)(t+s)} \, w_{kt}$$

$$A_6 = - \sum_{k=1}^{r} \sum_{t=0}^{\infty} [tk + (r - k)(t + s)]^2 \, b_{(r-k)t} \, w_{k(t+s)}$$

$$A_7 = \sum_{k=1}^{r} \sum_{t=1}^{\infty} [(t + s)k + (r - k)t]^2 \, b_{(r-k)(t+s)} \, w_{kt}$$

$$A_8 = - \sum_{k=0}^{\infty} \sum_{t=1}^{s} [(s - t)(k + r) + tk]^2 \, b_{k(s-t)} \, w_{(k+r)t}$$

$$A_9 = \sum_{k=1}^{\infty} \sum_{t=1}^{s} [(s - t)k + t(k + r)]^2 \, b_{(k+r)(s-t)} \, w_{kt}$$

The equations for $A_{o_1} \ldots A_{o_9}$ are the same as those for $A_1 \ldots A_9$, respectively, except that the b terms are replaced by b_o terms.

By integration the function F is found to satisfy the conditions

$$\int_o^b \sigma'_x \, dy = \int_o^b -\frac{\partial^2 F}{\partial y^2} \, dy = \bar{\sigma}_a b$$

for $x = 0$ and $x = a$ and

$$\int_o^a \sigma'_y \, dx = \int_o^a -\frac{\partial^2 F}{\partial x^2} \, dx = \bar{\sigma}_b a$$

for $y = 0$ and $y = b$

The remaining conditions that the solution must satisfy are that the edges $x = 0$, $x = a$, $y = 0$, and $y = b$ remain straight. These conditions require that $a\bar{\epsilon}_a$ be independent of y and that $b\bar{\epsilon}_b$ be independent of x. By actual evaluation, it is found that

$$\left.\begin{aligned} a\bar{\epsilon}_a &= \frac{\bar{\sigma}_a a}{E} - \frac{\mu\bar{\sigma}_b a}{E} + \frac{\pi^2}{8a}\sum_{m=1}^{\infty}\sum_{n=1}^{\infty} m^2 \left[w_{mn}^2 - \left(w_{o_{mn}}\right)^2\right] \\ b\bar{\epsilon}_b &= \frac{\bar{\sigma}_b b}{E} - \frac{\mu\bar{\sigma}_a b}{E} + \frac{\pi^2}{8b}\sum_{m=1}^{\infty}\sum_{n=1}^{\infty} n^2 \left[w_{mn}^2 - \left(w_{o_{mn}}\right)^2\right] \end{aligned}\right\} \quad (A12)$$

These expressions for $\bar{\epsilon}_a$ and $\bar{\epsilon}_b$ are independent of both x and y.

APPENDIX B

APPLICATION TO SQUARE PLATE

The formulas required for numerical work are given for the special case of a square plate subjected to compression in only one direction. Let

$$a = b$$

$$p_z = 0$$

$$\bar{\sigma}_b = 0$$

$$\mu = 0.316$$

The system of equations (A11) becomes simplified in this case to

$$0 = \frac{1}{10.8}\left(K_{rs} - K_{o_{rs}}\right)\left(r^2 + s^2\right)^2 - \frac{\bar{\sigma}_a}{\sigma_{cr_x}}\frac{r^2}{2.7}K_{rs} + \frac{1}{4Et^3}\left(A_{rs} - A_{o_{rs}}\right) \qquad (B1)$$

When symmetrical initial curvature and symmetrical buckling are assumed, and when only the first six components of the double harmonic series with odd subscripts are considered, K_{11}, K_{13}, K_{31}, K_{33}, K_{15}, K_{51} may be determined from six equations of the type of equation (A11) when $\bar{\sigma}_a/\sigma_{cr_x}$ and the initial curvature are known. These equations are similar to those in table II of reference 1.

Extreme-fiber strains.- From equations (A6), (A7), and (A10), the extreme-fiber strains at the plate center are given by

$$\left.\begin{aligned}
\frac{\epsilon_1}{\epsilon_{cr_x}} = \frac{\bar{\sigma}_a}{\sigma_{cr_x}} &+ 3(1-\mu^2)\sum_{p=0}^{\infty}\sum_{q=0}^{\infty}\frac{q^2}{Et^2}\left(b_{pq}-b_{o_{pq}}\right)(-1)^{\frac{p+q}{2}} \\
&- 3\mu(1-\mu^2)\sum_{p=0}^{\infty}\sum_{q=0}^{\infty}\frac{p^2}{Et^2}\left(b_{pq}-b_{o_{pq}}\right)(-1)^{\frac{p+q}{2}} \\
&+ 1.5(1-\mu^2)\sum_{m=1,3,5}^{\infty}\sum_{n=1,3,5}^{\infty}(-1)^{\left(\frac{m+n}{2}-1\right)}m^2\left(K_{mn}-K_{o_{mn}}\right) \\
\frac{\epsilon_2}{\epsilon_{cr_x}} = \frac{\bar{\sigma}_a}{\sigma_{cr_x}} &+ 3(1-\mu^2)\sum_{p=0}^{\infty}\sum_{q=0}^{\infty}\frac{q^2}{Et^2}\left(b_{pq}-b_{o_{pq}}\right)(-1)^{\frac{p+q}{2}} \\
&- 3\mu(1-\mu^2)\sum_{p=0}^{\infty}\sum_{q=0}^{\infty}\frac{p^2}{Et^2}\left(b_{pq}-b_{o_{pq}}\right)(-1)^{\frac{p+q}{2}} \\
&- 1.5(1-\mu^2)\sum_{m=1,3,5}^{\infty}\sum_{n=1,3,5}^{\infty}(-1)^{\left(\frac{m+n}{2}-1\right)}m^2\left(K_{mn}-K_{o_{mn}}\right)
\end{aligned}\right\} \quad (B2)$$

The difference of the extreme-fiber strains $\epsilon_1 - \epsilon_2$ in the x-direction at the center of the plate divided

by ϵ_{cr_x} is given by the following equation:

$$\frac{\epsilon_1 - \epsilon_2}{\epsilon_{cr_x}} = 3(1 - \mu^2) \sum_{m=1,3,5}^{\infty} \sum_{n=1,3,5}^{\infty} (-1)^{\left(\frac{m+n}{2}-1\right)} m^2 \left(K_{mn} - K_{o_{mn}}\right) \quad (B3)$$

Lateral deflection.- The deflection at the center of the plate divided by the plate thickness t is

$$\frac{\delta}{t} = \sum_{m=1,3,5}^{\infty} \sum_{n=1,3,5}^{\infty} (-1)^{\left(\frac{m+n}{2}-1\right)} K_{mn} \quad (B4)$$

The net deflection at the center of the plate divided by the plate thickness t is

$$\frac{\delta - \delta_o}{t} = \sum_{m=1,3,5}^{\infty} \sum_{n=1,3,5}^{\infty} (-1)^{\left(\frac{m+n}{2}-1\right)} \left(K_{mn} - K_{o_{mn}}\right) \quad (B5)$$

Effective width.- If a flat plate shortens without buckling, the average stress is $E\bar{\epsilon}_a$. The average stress on a buckled plate or a plate with initial curvature is $\bar{\sigma}_a$, which is less than $E\bar{\epsilon}_a$. In other words, the buckled plate or the plate with an initial deviation from flatness is equivalent in load-carrying capacity to a flat and unbuckled plate of the same thickness but smaller width. The width of this hypothetical plate, or the effective width b_e of the actual plate, can be obtained

by equating the load-carrying capacities of the two plates. Thus

$$E\bar{\epsilon}_a b_e t = \bar{\sigma}_a bt$$

Since, for elastic buckling,

$$E = \frac{\sigma_{cr_x}}{\epsilon_{cr_x}}$$

hence

$$b_e = \frac{\bar{\sigma}_a/\sigma_{cr_x}}{\bar{\epsilon}_a/\epsilon_{cr_x}} b \qquad (B6)$$

REFERENCES

1. Levy, Samuel: Bending of Rectangular Plates with Large Deflections. NACA TN No. 846, 1942.

2. Hoff, N. J.: Instability of Monocoque Structures in Pure Bending. Jour. R.A.S., vol. XLII, no. 328, April 1938, pp. 291-346.

3. Rossman, Carl A., Bartone, Leonard M., and Dobrowski, Charles V.: Compressive Strength of Flat Panels with Z-Section Stiffeners. NACA ARR No. 4B03, 1944.

4. Schuette, Evan H.: Charts for the Minimum-Weight Design of 24S-T Aluminum-Alloy Flat Compression Panels with Longitudinal Z-Section Stiffeners. NACA ARR No. L5F15, 1945.

5. Heimerl, George J., and Roy, J. Albert: Preliminary Report on Tests of 24S-t Aluminum-Alloy Columns of Z-, Channel, and H-Section That Develop Local Instability. NACA RB No. 3J27, 1943.

6. Lundquist, Eugene E., Schuette, Evan H., Heimerl, George J., and Roy, J. Albert: Column and Plate Compressive Strengths of Aircraft Structural Materials. 24S-T Aluminum-Alloy Sheet. NACA ARR No. L5F01, 1945.

7. Heimerl, George J., and Roy, J. Albert: Column and Plate Compressive Strengths of Aircraft Structural Materials. 17S-T Aluminum-Alloy Sheet. NACA ARR No. L5F08, 1945.

8. Heimerl, George J., and Roy, J. Albert: Column and Plate Compressive Strengths of Aircraft Structural Materials. Extruded 75S-T Aluminum Alloy. NACA ARR No. L5F08a, 1945.

9. Heimerl, George J., and Roy, J. Albert: Column and Plate Compressive Strengths of Aircraft Structural Materials. Extruded 24S-T Aluminum Alloy. NACA ARR No. L5F08b, 1945.

10. Heimerl, George J., and Fay, Douglas P.: Column and Plate Compressive Strengths of Aircraft Structural Materials. Extruded R303-T Aluminum Alloy. NACA ARR No. L5H04, 1945.

11. Southwell, R. V.: On the Analysis of Experimental Observations in Problems of Elastic Stability. Proc. Roy. Soc. (London), ser. A, vol. 135, April 1, 1932, pp. 601-616.

12. Lundquist, Eugene E.: Generalized Analysis of Experimental Observations in Problems of Elastic Stability. NACA TN No. 658, 1938.

13. Timoshenko, S.: Theory of Elastic Stability. McGraw-Hill Book Co., Inc., 1936.

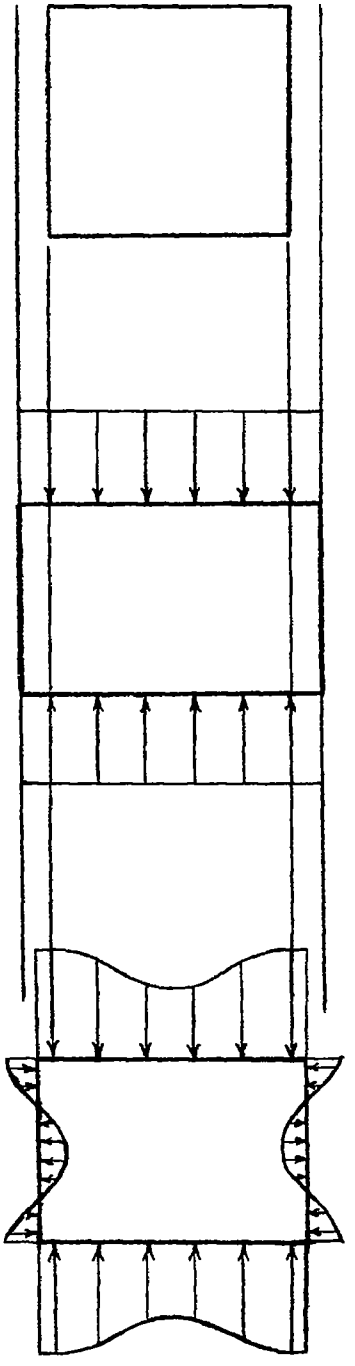

(a) Before loading.

(b) After loading; just before buckling.

(c) After buckling.

NATIONAL ADVISORY
COMMITTEE FOR AERONAUTICS

Figure 1.- Edge-stress distribution for a simply supported flat plate under edge compression.

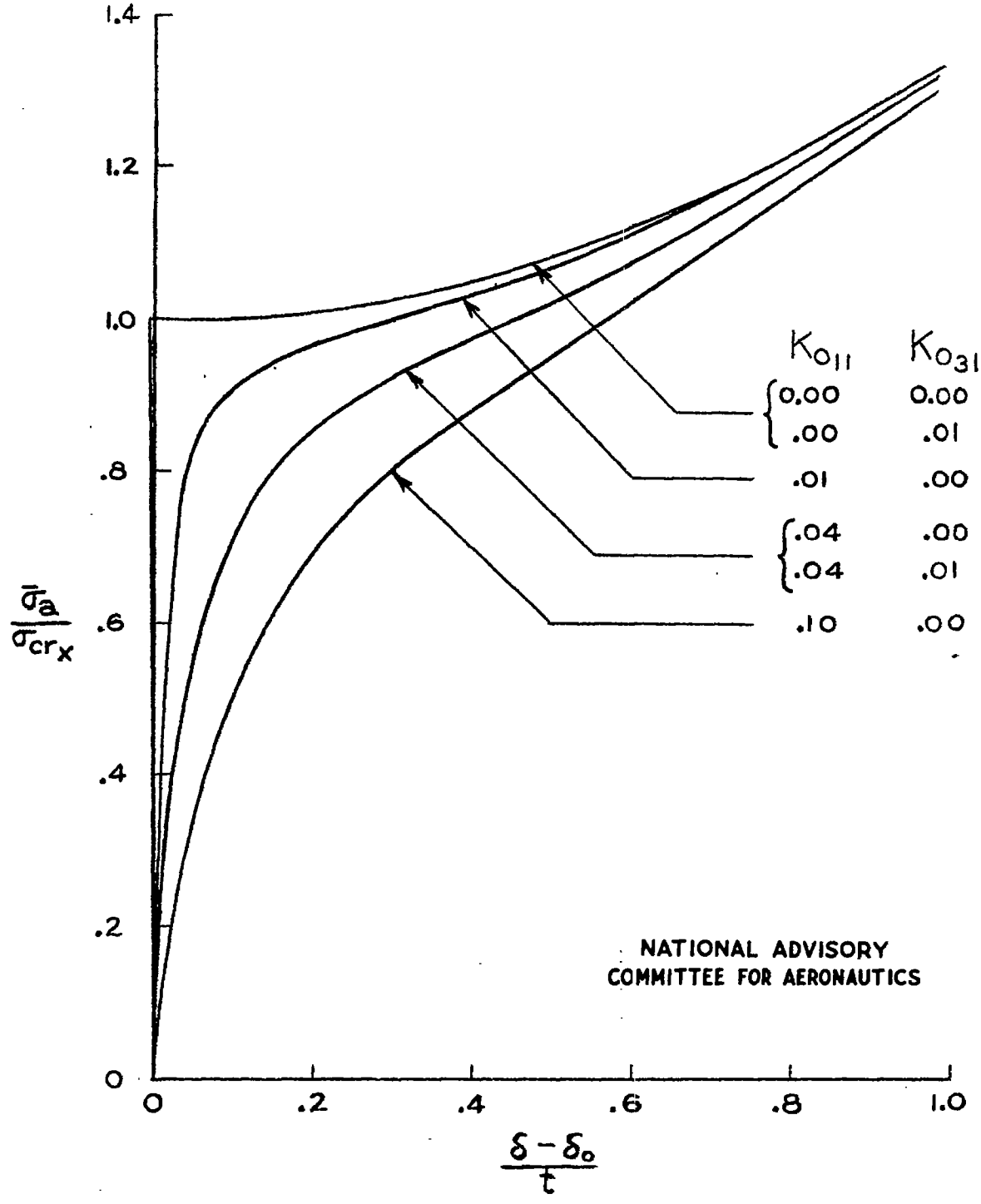

Figure 2.- Variation of net-center-deflection ratio with average edge-compressive-stress ratio for simply supported square plates with slight initial deviations from flatness.

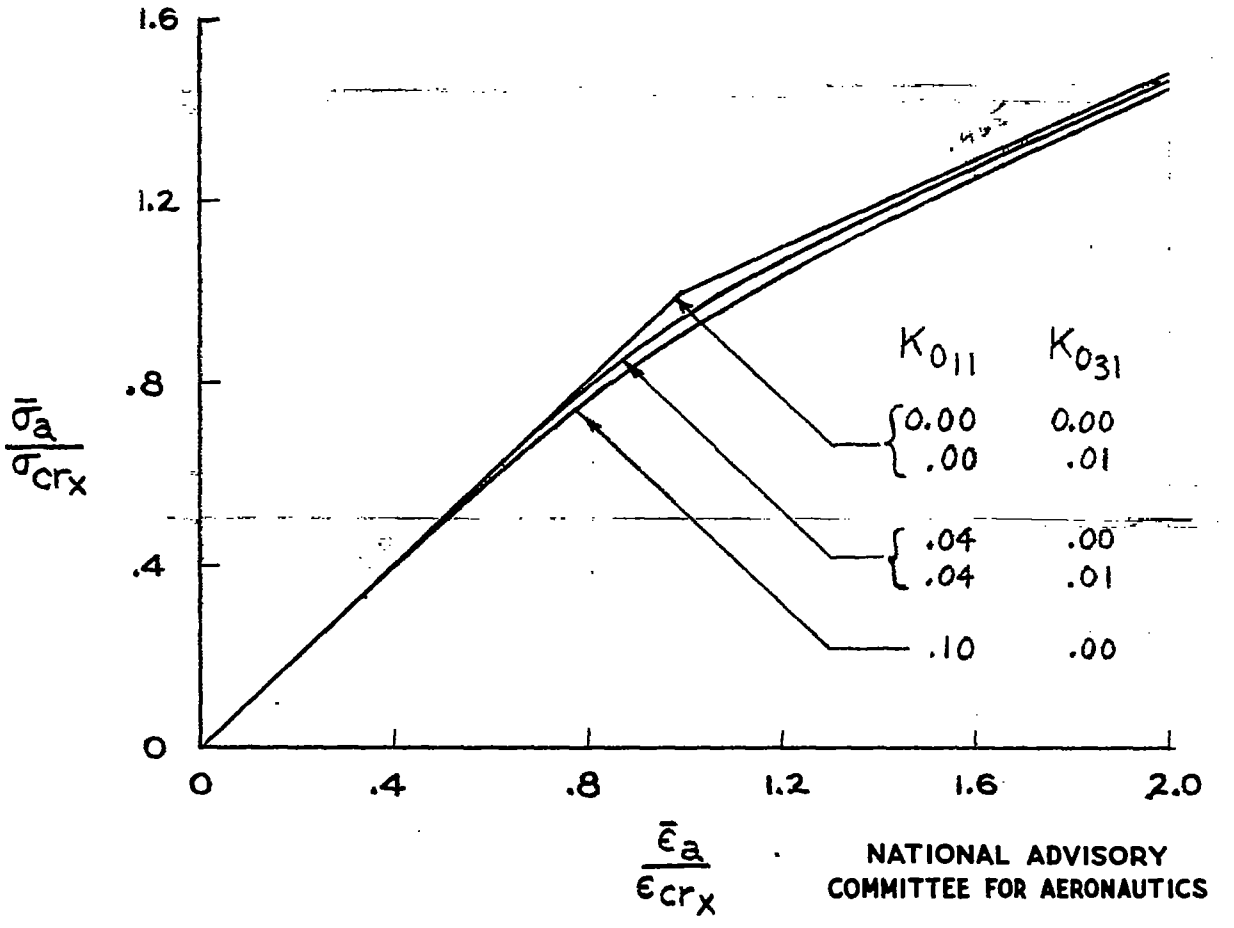

Figure 3.- Variation of unit-plate-shortening ratio with average edge-compressive-stress ratio for simply supported square plates with slight initial deviations from flatness.

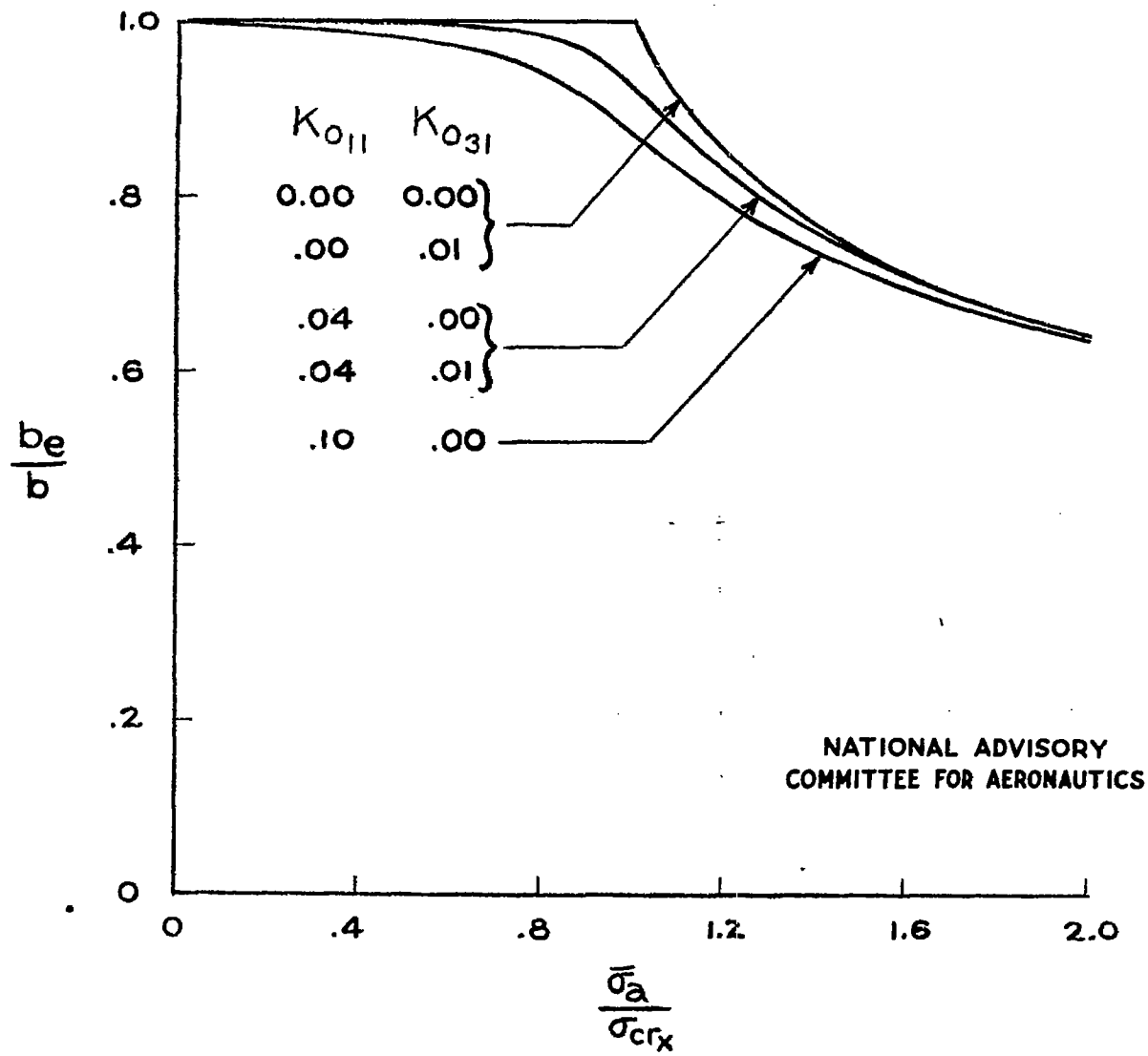

Figure 4.- Variation of effective-width ratio for load-carrying capacity with average edge-compressive-stress ratio for simply supported square plates with slight initial deviations from flatness.

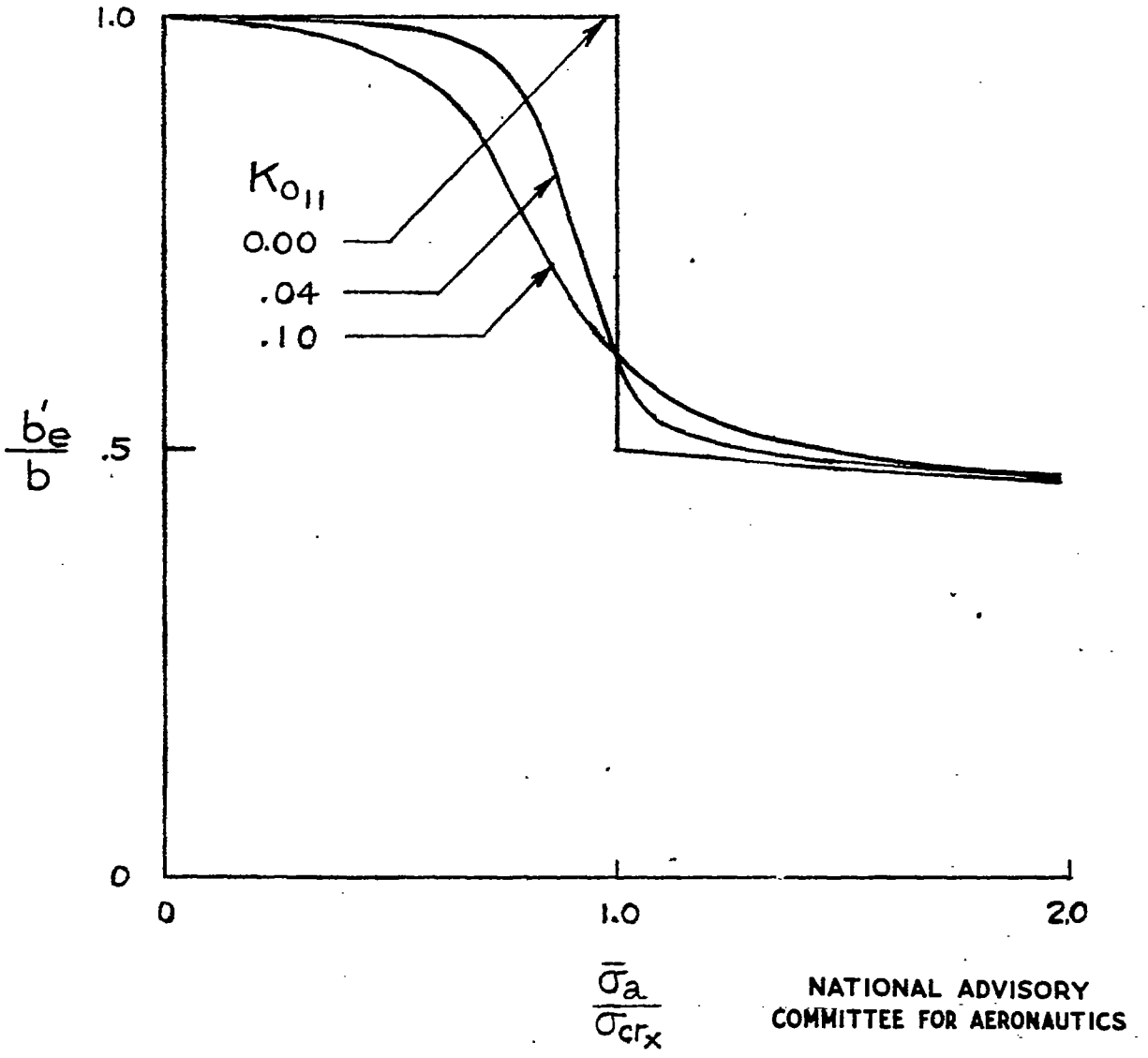

Figure 5.- Variation of effective-width ratio for stiffness with average edge-compressive-stress ratio for simply supported square plates with slight initial deviations from flatness.

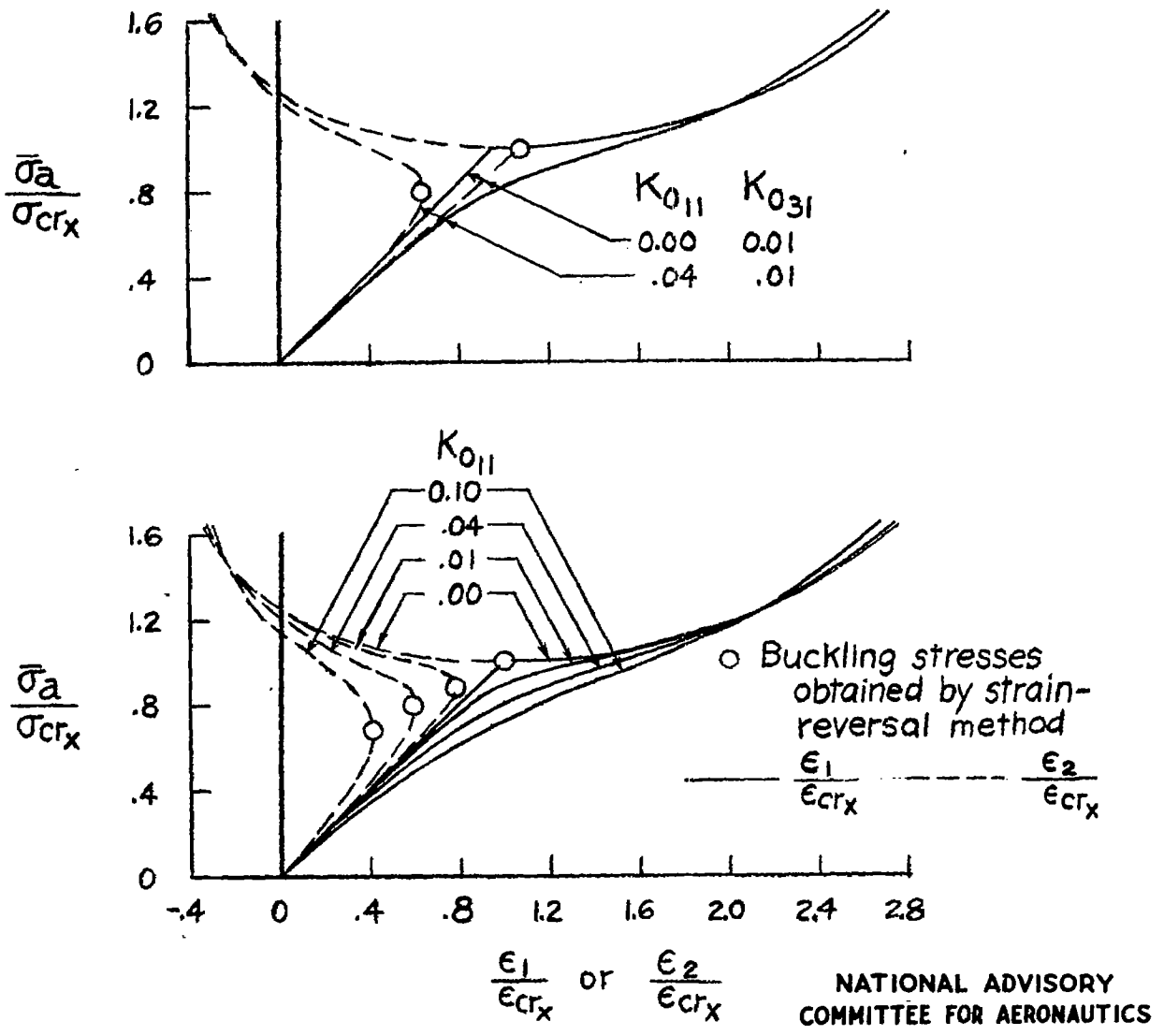

Figure 6.- Variation of extreme-fiber-strain ratios at plate center with average edge-compressive-stress ratio for simply supported square plates with slight initial deviations from flatness.

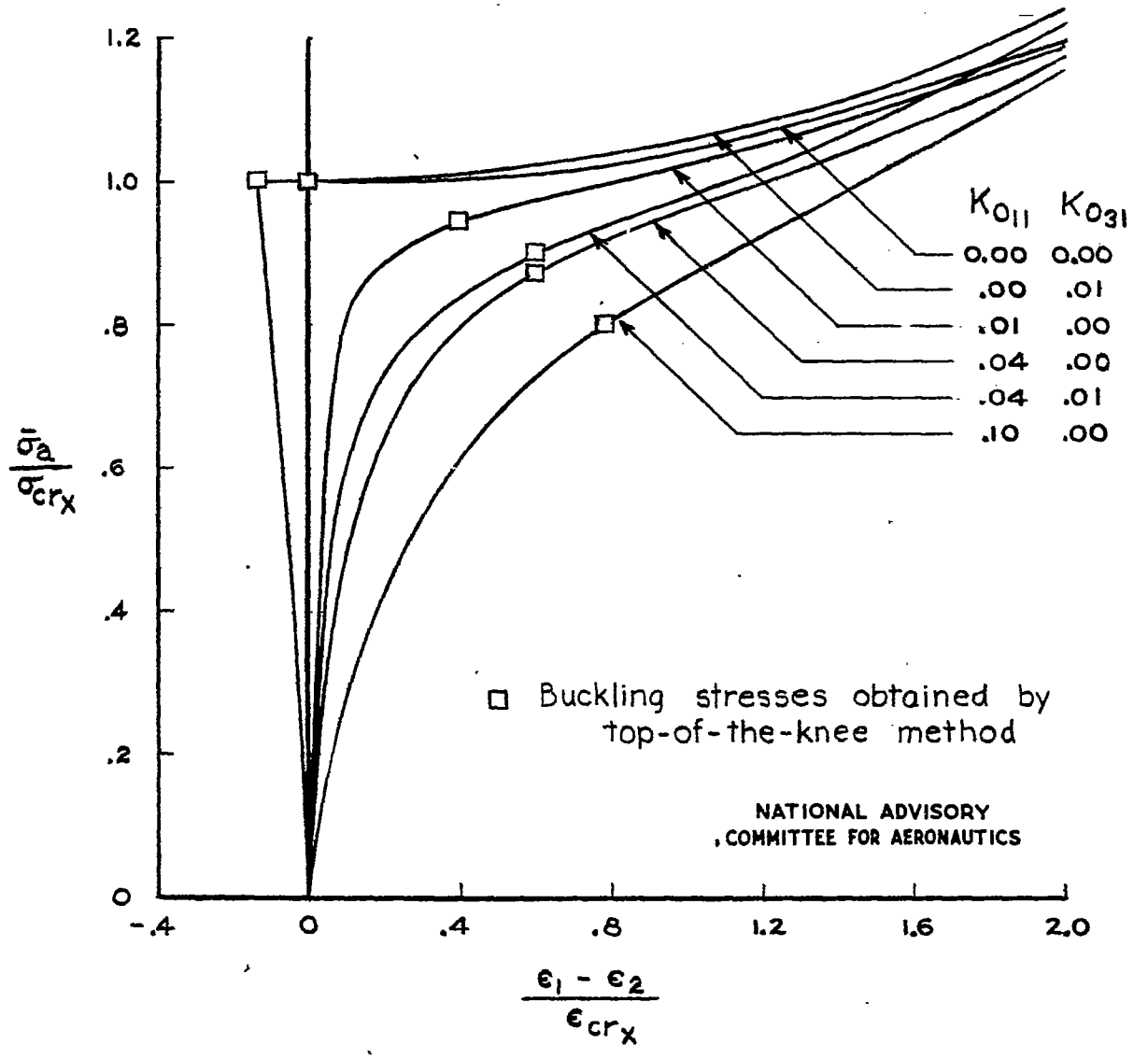

Figure 7.- Variation of difference in extreme-fiber-strain ratios at plate center with average edge-compressive-stress ratio for simply supported square plates with slight initial deviations from flatness.

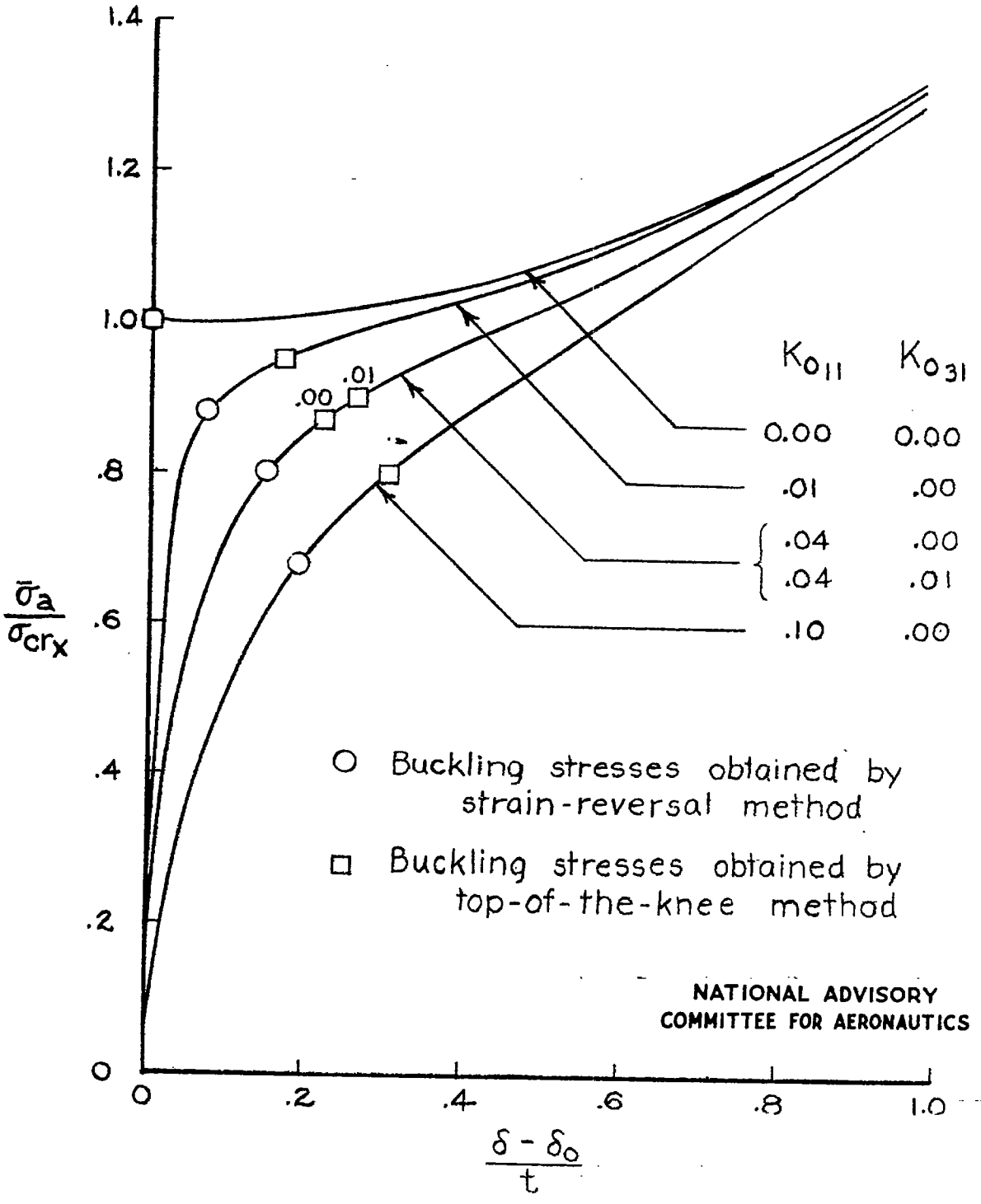

Figure 8.- Comparison of buckling-stress ratios obtained by strain-reversal method and top-of-the-knee method.

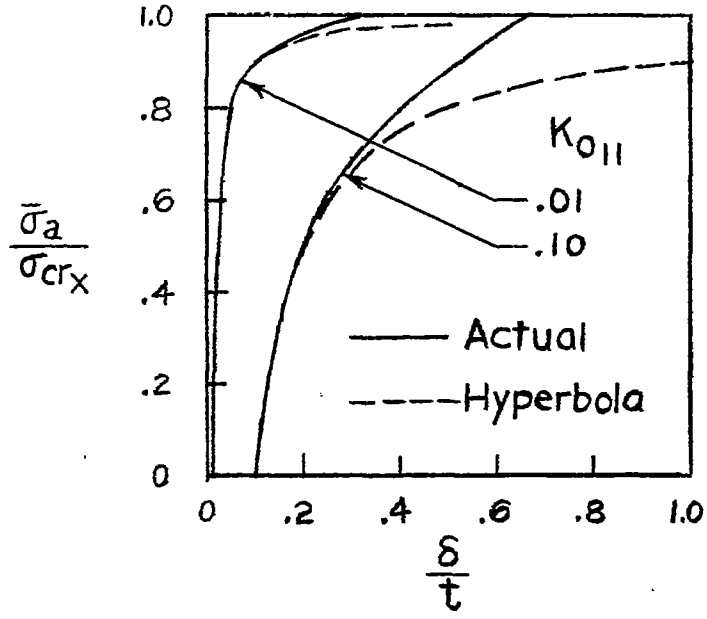

(a) Plates.

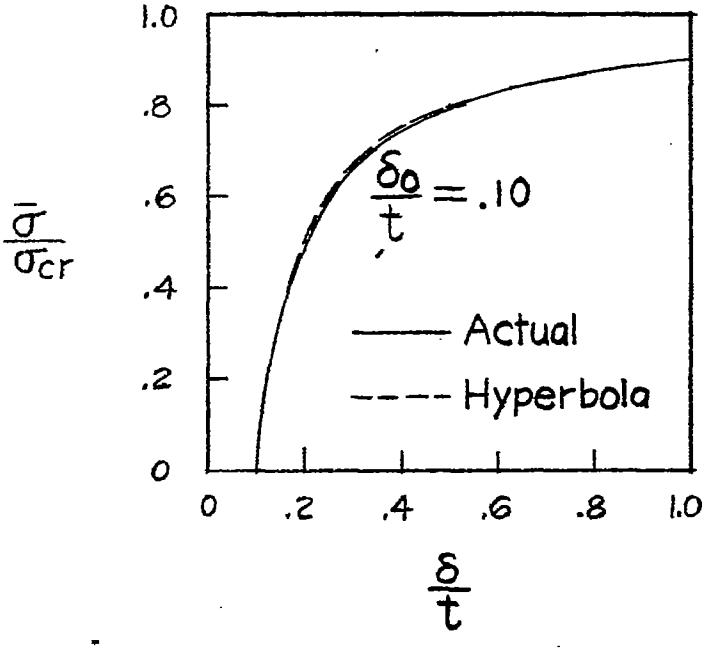

(b) Rectangular column with initial shape of circular arc. Length = 30t.

NATIONAL ADVISORY COMMITTEE FOR AERONAUTICS

Figure 9.- Comparison of calculated stress-deflection curves for simply supported columns and plates with the rectangular hyperbolas that the curves must closely approximate if the Southwell plot method is to apply.

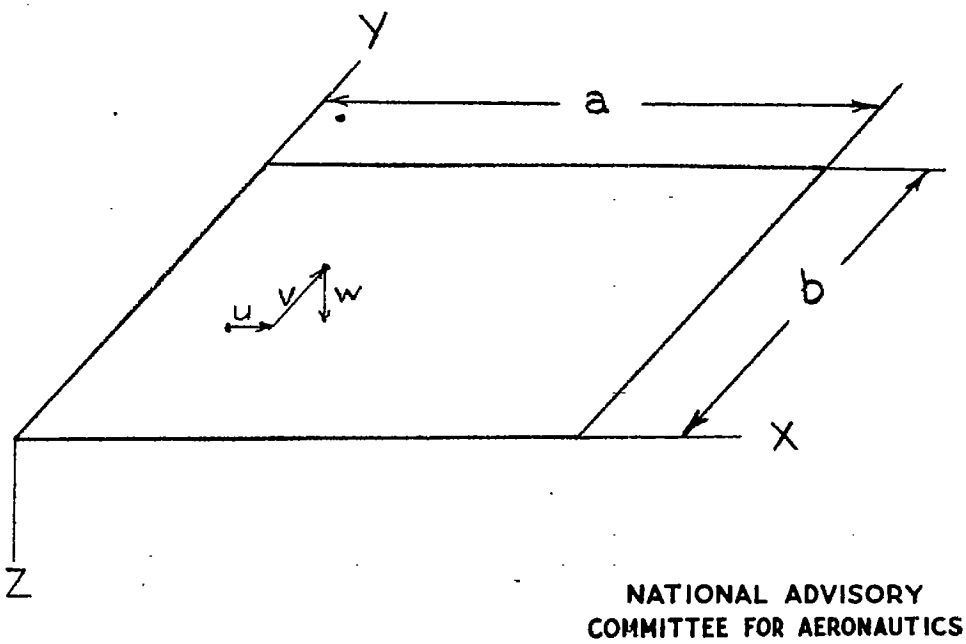

Figure 10.- Coordinate system for rectangular plate.